Atom-Molecule Dark States in a Bose-Einstein Condensate

K. Winkler,[1] G. Thalhammer,[1] M. Theis,[1] H. Ritsch,[2] R. Grimm,[1,3] and J. Hecker Denschlag[1]

[1]*Institut für Experimentalphysik, Universität Innsbruck, 6020 Innsbruck, Austria*

[2]*Institut für Theoretische Physik, Universität Innsbruck, 6020 Innsbruck, Austria*

[3]*Institut für Quantenoptik und Quanteninformation, Österreichische Akademie der Wissenschaften, 6020 Innsbruck, Austria*

(Received 30 May 2005; published 5 August 2005)

We have created a dark quantum superposition state of a Rb Bose-Einstein condensate and a degenerate gas of Rb_2 ground-state molecules in a specific rovibrational state using two-color photoassociation. As a signature for the decoupling of this coherent atom-molecule gas from the light field, we observe a striking suppression of photoassociation loss. In our experiment the maximal molecule population in the dark state is limited to about 100 Rb_2 molecules due to laser induced decay. The experimental findings can be well described by a simple three mode model.

DOI: 10.1103/PhysRevLett.95.063202 PACS numbers: 34.50.Rk, 03.75.Nt, 32.80.Pj, 42.50.Gy

The phenomenon of coherent dark states is well known in quantum optics and is based on a superposition of long-lived system eigenstates which decouple from the light field. Since their discovery [1] dark states have found numerous applications. Prominent examples are electromagnetically induced transparency and lasing without inversion [2], subrecoil laser cooling [3], and ultrasensitive magnetometers [4]. A particular application is the coherent transfer of population between two long-lived states by a stimulated Raman adiabatic passage (STIRAP) [5].

In the emerging field of ultracold molecules, the conversion of atomic into molecular Bose-Einstein condensates (BECs) is a central issue. A series of recent experiments on the creation of molecular quantum gases rely on the application of Feshbach resonances [6]. This coupling mechanism, however, is restricted to the creation of molecules in the highest rovibrational level and is only practicable for a limited number of systems. As a more general method, a stimulated optical Raman transition can directly produce deeply bound molecules as demonstrated a few years ago [7,8]. STIRAP was proposed as a promising way for a fast, efficient, and robust process to convert a BEC of atoms into a molecular condensate [9–15]. The central prerequisite for this kind of STIRAP is a dark superposition state of a BEC of atoms and a BEC of molecules.

In this Letter, we report the observation of such a collective multiparticle dark state in which atoms in a BEC are pairwise coupled coherently to ground-state molecules. This dark atom-molecule BEC shows up in a striking suppression of photoassociative loss, as illustrated by the spectra in Fig. 1. In one-color photoassociation, the excitation of a molecular transition produces a resonant loss feature that reflects the optical transition linewidth; see Fig. 1(a). The presence of a second laser field coupling the electronically excited molecular state to a long-lived ground-state level can drastically reduce this loss, as shown in Fig. 1(b) and 1(c). In Fig. 1(b), for example, we observe a striking loss suppression by about a factor of 70 on resonance.

Already the mere observation of an atom-molecule dark resonance in a BEC proves that a coherent, quantum degenerate gas of molecules has been formed. This follows from the facts that (1) the dark state is by definition a coherent superposition of atoms and molecules and (2) the atomic BEC is a coherent matter wave. In this fully coherent situation, the molecular fraction itself must be quantum degenerate with a phase-space density corresponding to the number of molecules. The very narrow resonance lines indicate the high resolution of our measurements and the potential sensitivity of the dark state as an analysis tool. Using a BEC allows direct interpretation

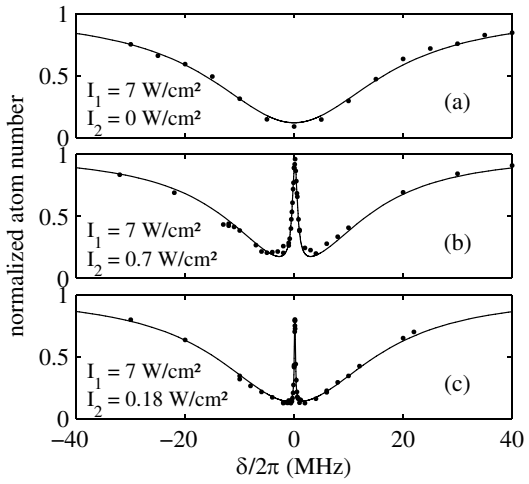

FIG. 1. Dark resonances in two-color photoassociation. (a) Atomic loss signal in one-color photoassociation as a function of the laser detuning from the electronically excited molecular line. (b), (c) When we apply a second laser (fixed frequency) which resonantly ($\Delta = 0$) couples the excited molecular state to a long-lived molecular ground state, the losses are strongly suppressed at $\delta = 0$. Depending on the intensity of laser 2, this dark resonance can get very narrow. The atom lifetime on the dark resonance in (b) is 140 ms whereas in (a) atoms have an initial decay time of about 2 ms. Intensities of laser 1 (I_1) and 2 (I_2) are as indicated.

and clear understanding of our data without ambiguity. Thermal averaging of signal features plays no role in contrast to previous measurements in thermal gases [8,16,17].

The starting point of our measurements is a BEC of 4×10^5 ^{87}Rb atoms in the spin state $|F = 1, m_F = -1\rangle$ [18]. In the level scheme of Fig. 2 the atomic BEC state is represented by $|a\rangle$. Laser 1 couples this state to the excited molecular state $|b\rangle$. Laser 2 couples $|b\rangle$ to the molecular ground state $|g\rangle$. We choose level $|b\rangle$ to be the electronically excited molecular state $|0_g^-, v = 1, J = 2\rangle$ located 26.8 cm^{-1} below the $S_{1/2} + P_{3/2}$ dissociation asymptote [18]. For level $|g\rangle$ we choose the second to last bound state in the ground-state potential. It has a binding energy of $E_b/h = 636$ MHz [7]. $|a\rangle$, $|b\rangle$, and $|g\rangle$ form the lambda system for the atom-molecule dark states.

We illuminate the trapped condensate for typically 10 ms with two phase-locked laser beams in a Raman configuration as shown in Fig. 2. Both laser beams are derived either from a single diode laser or, for higher optical powers, from a Ti:sapphire laser. The frequency difference between the two beams is created with an acousto-optical modulator at a center frequency of about 320 MHz in a double-pass configuration. This allows precise control of the beams' relative frequency difference over several tens of MHz. Both beams propagate collinearly and are aligned along the weak axis of the trap. They have a waist of about 100 μm, and their linear polarization is perpendicular to the magnetic bias field of the trap. The diode laser and the Ti:sapphire laser both have linewidths of less than 1 MHz. They are offset locked relative to the D_2 line of atomic rubidium with the help of a scanning optical cavity. This yields an absolute frequency stability of better than 10 MHz.

We are able to describe all of our spectra with a relatively simple three-mode model. Although the atom-molecule dark states are intrinsically complicated and entangled, in a first approximation the atoms and molecules can be represented as coherent matter fields [9–15]. Using the notation of Mackie *et al.* [11] we obtain a set of differential equations for the normalized field amplitudes a, b, and g of the BEC state, the excited molecular and ground state, respectively:

$$i\dot{a} = -\Omega_1 a^* b, \tag{1a}$$

$$i\dot{b} = [(\Delta + \delta) - i\gamma_b/2]b - \tfrac{1}{2}(\Omega_1 aa + \Omega_2 g), \tag{1b}$$

$$i\dot{g} = (\delta - i\gamma_g/2)g - \tfrac{1}{2}\Omega_2 b. \tag{1c}$$

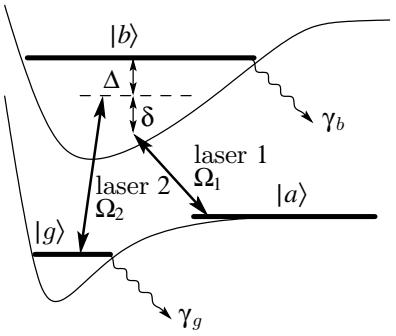

FIG. 2. Level scheme. Δ and δ denote the detunings. Ω_1 and Ω_2 are the Rabi frequencies. The excited molecular state $|b\rangle$ spontaneously decays with a rate γ_b to levels outside this scheme. The molecular state $|g\rangle$ is attributed a decay rate γ_g which phenomenologically takes into account losses through inelastic collisions and laser induced dissociation, e.g., when laser 1 couples $|g\rangle$ to the unstable state $|b\rangle$. In all our measurements laser 1 is scanned (varying δ) while laser 2 is held fixed at a particular detuning Δ.

We refer to Ω_1 as the free-bound Rabi frequency (see Fig. 2). It scales with intensity I_1 of laser 1 and initial atom density ρ as $\Omega_1 \propto \sqrt{I_1}\sqrt{\rho}$, where the factor $\sqrt{\rho}$ follows directly from the transition matrix element of a free-bound transition [13]. The bound-bound Rabi frequency $\Omega_2 \propto \sqrt{I_2}$ only depends on the intensity I_2 of laser 2. The detunings Δ and δ are defined as depicted in Fig. 2. γ_b and γ_g denote the effective decay rates of state $|b\rangle$ and $|g\rangle$ (for details, see Fig. 2). $|a|^2$, $|b|^2$ and $|g|^2$ give the ratio between the respective atom (molecule) number and the initial atom number. In the absence of losses, i.e., $\gamma_b = \gamma_g = 0$, particle numbers are conserved globally, $|a|^2 + 2|b|^2 + 2|g|^2 = 1$. Unlike the previous theoretical treatments [9–15] where the decay rate γ_g was basically neglected, we find that γ_g is relatively large and intensity dependent, $\gamma_g = \gamma_g(I_1)$. In our simple model we do not include atomic continuum states other than the BEC state. We neglect inhomogeneity effects due to the trapping potentials and finite size laser beams. Energy shifts caused by the mean-field interaction of atoms and molecules are small and neglected.

In order to determine the parameters of our model and to check it for consistency, we performed measurements in a broad parameter range of intensities and detunings. Fits to the photoassociation curves determine all unknown parameters of the system such as Ω_1, Ω_2, γ_b, and γ_g. Figure 3 shows photoassociation spectra for a relatively high laser power $I_2 = 20$ W/cm^2 and various detunings Δ. For a small detuning Δ [Fig. 3(a)] the dark resonance line from Fig. 1 has broadened considerably. This spectrum can also be viewed as two absorption lines resulting from a strong Autler-Townes splitting which was also observed in thermal gases [8,17]. From the 30 MHz separating the two resonance dips, the magnitude of the Rabi frequency Ω_2 can be directly determined. For a larger detuning Δ, the resulting spectrum becomes asymmetric and turns into a narrow and a broad dip; see Fig. 3(b) and 3(c). The narrow loss feature is related to the two-photon Raman transition while the broad dip is due to the one-photon transition $|a\rangle \rightarrow |b\rangle$. Note that similar to Fig. 1, losses are suppressed at $\delta = 0$.

Figure 4 shows the dark resonances in the low power limit where I_1 is held constant and I_2 is lowered in 4 steps.

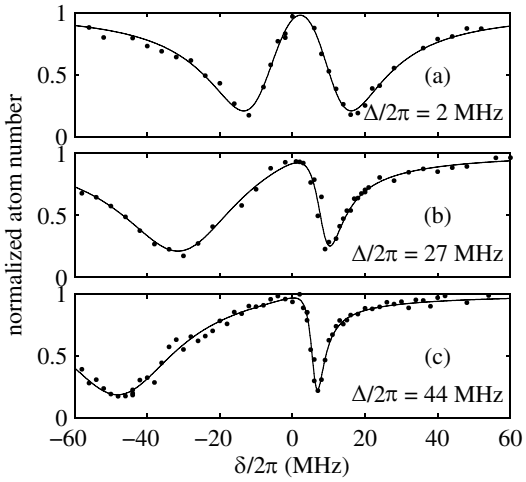

FIG. 3. Two-color photoassociation spectra for various detunings Δ at a large intensity $I_2 = 20\ \mathrm{W/cm^2}$. Here $I_1 = 80\ \mathrm{W/cm^2}$. The solid lines are fit curves based on our theoretical model.

The dark state transforms more and more into a gray state, because losses become more dominant due to a nonzero decay rate γ_g. The height of the dark resonance decreases when the pumping rate Ω_2^2/γ_b comes in the range of the decay rate of the molecular ground state γ_g. This allows for a convenient determination of γ_g. From Fig. 4 it is also clear that the width of the dark resonance decreases with Ω_2. For $\Omega_2 \ll \gamma_b$ the width is given by $\Omega_2^2/\gamma_b + \gamma_g$, corresponding to power broadening and the effective ground-state relaxation. The following set of parameters describes all our measurements quite accurately. It was used, in particular, for the calculated solid lines in Fig. 4 and it is consistent with previous measurements [18]: $\Omega_1/(\sqrt{I_1}\sqrt{\rho/\rho_0}) = 2\pi \times 8\ \mathrm{kHz/(W\,cm^{-2})^{1/2}}$ at a peak density of $\rho_0 = 2 \times 10^{14}\ \mathrm{cm^{-3}}$, $\Omega_2/\sqrt{I_2} = 2\pi \times 7\ \mathrm{MHz/(W\,cm^{-2})^{1/2}}$, and $\gamma_b = 2\pi \times 13$ MHz. We find that the decay rate γ_g of the ground-state molecular level increases with the intensity I_1 of laser 1 as shown in Fig. 5. A dependence of γ_g on I_2 was negligible in our experiments where typically $I_2/I_1 \sim 1/5 \ldots 1/500$. We model the behavior of γ_g as $\gamma_g = 2\pi \times 6\ \mathrm{kHz/(W\,cm^{-2})} I_1 + \gamma_{\mathrm{bg}}$, the sum of a light-induced decay rate proportional to I_1 and a background decay rate γ_{bg} due to inelastic collisions in the absence of light. From measurements at low intensities we can estimate an upper value for the background decay rate of about $\gamma_{\mathrm{bg}} \approx 2\pi \times 1$ kHz for $\rho_0 = 2 \times 10^{14}\ \mathrm{cm^{-3}}$. This value for γ_{bg} is consistent with previous experimental results for ^{87}Rb at similar atom densities [7]. The increase of γ_g with I_1 is due to several imperfections which break the ideal three-level lambda system. Laser 1 also couples the molecular ground state $|g\rangle$ to the short-lived excited molecular state $|b\rangle$, which leads to an incoherent loss of the molecules due to spontaneous decay. Because of the rather small frequency difference ($\approx 2\pi \times 636$ MHz) of the two Raman lasers and the strong bound-bound transition, this cannot be neglected. In addition, only 290 MHz below level $|b\rangle$ exists another excited molecular state $|0_g^-, v = 1, J = 0\rangle$ which represents an additional loss channel [18]. These two contributions explain about one third of our observed losses. Furthermore, losses can also stem from a photodissociation transition which couples ground-state molecules directly to the continuum above the $S_{1/2} + P_{1/2}$ dissociation asymptote.

Having determined the parameters we can use model (1) to calculate the fraction of ground-state molecules $|g|^2$. For the measurements presented in Fig. 4 we have a peak molecular fraction of 2×10^{-4} corresponding to about 100 molecules (at $\delta = 0$ and $I_2/I_1 = 1/500$). For comparison, for $I_2/I_1 = 1/40$ the molecule number is only about 25 at $\delta = 0$. It is interesting to note how few molecules are needed to stabilize almost a million atoms against photoassociation. This large asymmetry of the particle numbers reflects the different coupling strengths of the free-bound and bound-bound transitions. Naturally the question arises how the experimental parameters should be chosen to optimize the number of molecules. This is nontrivial due to the finite decay rate γ_g. With model (1) we have numerically mapped out molecule numbers as a function of time, detuning, and laser intensities, starting

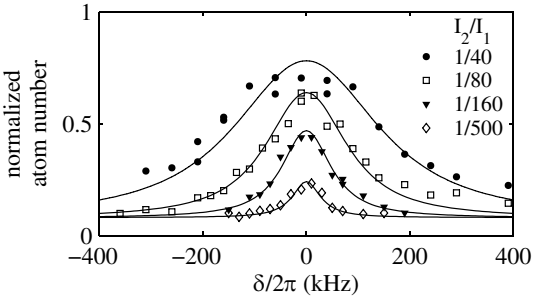

FIG. 4. Dark resonances [blowup of the central part of Fig. 1(c) and similar curves] for different intensity ratios I_2/I_1 (see legend) at a fixed intensity $I_1 = 7\ \mathrm{W/cm^2}$. The solid curves are calculations based on our theoretical model. $\Delta = 0$.

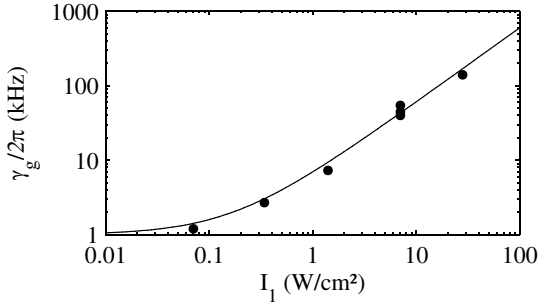

FIG. 5. Dependence of the decay rate γ_g of the ground-state molecules on the laser intensity I_1, measured with an intensity ratio $I_2/I_1 = 1/40$. The solid curve is given by $\gamma_g = 2\pi \times 6\ \mathrm{kHz/(W\,cm^{-2})} I_1 + 2\pi \times 1$ kHz.

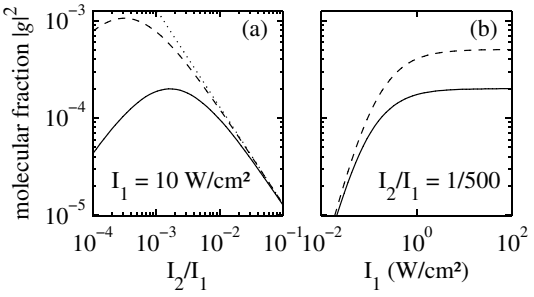

FIG. 6. (a) Maximum molecular fraction as function of the intensity ratio I_2/I_1 at a fixed intensity $I_1 = 10\ \mathrm{W/cm^2}$ and (b) as a function of intensity I_1 at a fixed intensity ratio $I_2/I_1 = 1/500$. The solid lines show the molecule fraction for the measured decay rate $\gamma_g = 2\pi \times 6\ \mathrm{kHz}/(\mathrm{W\,cm^{-2}})I_1 + \gamma_{\mathrm{bg}}$. The dashed lines show the molecule fraction assuming a lower decay rate $\gamma_g = 2\pi \times 1\ \mathrm{kHz}/(\mathrm{W\,cm^{-2}})I_1 + \gamma_{\mathrm{bg}}$. The dotted line corresponds to $\gamma_g = 0$. The calculations are based on Eqs. (1) with $\Delta = 0$.

out with a pure atomic BEC and simply switching on the lasers. In general, within a few μs of evolution, the dark state is formed. This involves only negligible losses of atoms since the dark state is very close to our initial BEC state. The maximum number of molecules of every evolution is then determined. We find that we can optimize the molecular production by working at $\Delta = 0$ although other values for Δ can be used. For $\Delta = 0$ the maximum number of molecules corresponds to $\delta = 0$, hence both lasers are on resonance. Figure 6 shows the molecular fraction as a function of the laser intensities. In Fig. 6(a), as I_2/I_1 is lowered from high values, the molecule fraction initially grows and follows a straight dotted line. Because of the finite γ_g the molecular fraction curve rolls over for some value of I_2/I_1, when the molecule loss rate is larger than its production rate. A smaller γ_g would lead to a larger number of molecules (dashed line). In the limit $\gamma_g = 0$ the molecular fraction is located on the dotted line. We note that for our parameter range, this line coincides with the ideal ($\gamma_g = 0$) route for a STIRAP conversion from atoms to molecules. The finite γ_g in our experiments leads to a maximum molecule number at $I_2/I_1 \sim 1/500$, a ratio which we also used in our measurements (see Fig. 4, open diamonds). For this optimum value the dependence of the molecular fraction on I_1 is shown in Fig. 6(b). Here it becomes clear that the laser intensities have to be kept above a certain threshold so that losses are not dominated by the background decay rate γ_{bg} of the molecular state.

To summarize, we have created a novel multiparticle dark state where an optical Raman transition coherently couples an atomic Rb BEC of about 4×10^5 atoms to a quantum degenerate gas of up to 100 Rb_2 ground-state molecules. Our investigations can be extended in a straight forward manner to create and study BECs of arbitrarily deeply bound molecules and coherent atom-molecule mixtures. The dark resonance has proven itself as a useful tool to analyze the atom-molecule system and to optimize the optical conversion of atomic to molecular BECs. An increase of the number of molecules by several orders of magnitude should be possible by choosing better suited ground and excited molecular states for the free-bound Raman transition.

We appreciate the help of George Ruff and Michael Hellwig at an early stage of the experiment. We thank Paul Julienne, Eite Tiesinga, Peter Drummond, and Karen Kheruntsyan for valuable discussions. This work was supported by the Austrian Science Fund (FWF) within SFB 15 (project parts 12 and 17) and the European Union in the frame of the Cold Molecules TMR Network under Contract No. HPRN-CT-2002-00290.

Note added.—Recently, atom-molecule dark states have also been observed in a sodium gas [19].

[1] E. Arimondo and G. Orriols, Lett. Nuovo Cimento Soc. Ital. Fis. **17**, 333 (1976).
[2] For a review, see, e.g., S. E. Harris, Phys. Today **50**, No. 7, 36 (1997).
[3] A. Aspect *et al.*, Phys. Rev. Lett. **61**, 826 (1988).
[4] M. Stähler *et al.*, Opt. Lett. **27**, 1472 (2002).
[5] K. Bergmann, H. Theuer, and B. W. Shore, Rev. Mod. Phys. **70**, 1003 (1998).
[6] For a review, see, e.g., D. Kleppner, Phys. Today **57**, No. 8, 12 (2004).
[7] R. Wynar, R. S. Freeland, D. J. Han, C. Ryu, and D. J. Heinzen, Science **287**, 1016 (2000).
[8] B. Laburthe Tolra, C. Drag, and P. Pillet, Phys. Rev. A **64**, 061401 (2001).
[9] A. Vardi, D. Abrashkevich, E. Frishman, and M. Shapiro, J. Chem. Phys. **107**, 6166 (1997); A. Vardi, V. A. Yurovsky, and J. R. Anglin, Phys. Rev. A **64**, 063611 (2001).
[10] P. S. Julienne, K. Burnett, Y. B. Band, and W. C. Stwalley, Phys. Rev. A **58**, R797 (1998).
[11] J. Javanainen and M. Mackie, Phys. Rev. A **58**, R789 (1998); M. Mackie, A. Collin, and J. Javanainen, Phys. Rev. A **71**, 017601 (2005).
[12] J. J. Hope, M. K. Olsen, and L. I. Plimak, Phys. Rev. A **63**, 043603 (2001).
[13] P. D. Drummond, K. V. Kheruntsyan, D. J. Heinzen, and R. H. Wynar, Phys. Rev. A **65**, 063619 (2002); **71**, 017602 (2005).
[14] B. Damski *et al.*, Phys. Rev. Lett. **90**, 110401 (2003).
[15] H. Y. Ling, H. Pu, and B. Seaman, Phys. Rev. Lett. **93**, 250403 (2004).
[16] C. Lisdat, N. Vanhaecke, D. Comparat, and P. Pillet, Eur. Phys. J. D **21**, 299 (2002).
[17] U. Schlöder, T. Deuschle, C. Silber, and C. Zimmermann, Phys. Rev. A **68**, 051403 (2003).
[18] For details, see, e.g., G. Thalhammer *et al.*, Phys. Rev. A **71**, 033403 (2005).
[19] R. Dumke, J. D. Weinstein, M. Johanning, K. M. Jones, and P. D. Lett, cond-mat/0508077.